

Repository Istituzionale dei Prodotti della Ricerca del Politecnico di Bari

Multiscale mechanics of macromolecular materials with unfolding domains

This is a pre-print of the following article

Original Citation:
Multiscale mechanics of macromolecular materials with unfolding domains / DE TOMMASI, D., Puglisi, G., Saccomandi, G.. - In: JOURNAL OF THE MECHANICS AND PHYSICS OF SOLIDS. - ISSN 0022-5096. - 78:(2015), pp. 154-172. [10.1016/j.jmps.2015.02.002]

Availability:
This version is available at http://hdl.handle.net/11589/773 since: 2022-06-05

Published version
DOI:10.1016/j.jmps.2015.02.002

Publisher:

Terms of use:

(Article begins on next page)

16 November 2026

https://www.sciencedirect.com/science/article/abs/pii/S0022509615000332
DOI: 10.1016/j.jmps.2015.02.002

A multiscale model for macromolecular materials with unfolding domains

D. De Tommasi[1,*], G. Puglisi[1,*], G. Saccomandi[1,**]

Abstract

We propose a simple approach, based on the minimization of the total (entropic plus unfolding) energy of a two-state system, to describe the unfolding of multidomains macromolecules (proteins, silks, polysaccharides, nanopolymers). The model is fully analytical and enlightens the role of the different energetic components regulating the unfolding evolution. As an explicit example we compare the analytical results with the titin Atomic Force Microscopy stretch-induced unfolding experiment showing the ability of the model to quantitatively reproduce the experimental behavior. In the thermodynamic limit the sawtooth force-elongation unfolding curve degenerates to a constant force unfolding plateau.

Keywords: Macromolecules unfolding, Biopolymers, Macromolecules Mechanics, Biological tissues, Multiscale models, Worm Like Chain.

1. Introduction

2. Micromechanics of the single chain unfolding

{ea}

Typical protein macromolecules are constituted by a sequence of folded (*e.g.* β-sheets crystals) and unfolded domains. Atomic Force Microscopy experiments (see [67] for the titin and [10] for fibrinogen, dextan [65], silks [83],

*Dipartimento di Scienze dell'Ingegneria Civile e dell'Architettura
Politecnico di Bari, Bari
**Dipartimento di Ingegneria Industriale, Università degli Studi di Perugia
Email addresses: d.detommasi@poliba.it (D. De Tommasi), g.puglisi@poliba.it (G. Puglisi), zurlo@lms.polytechnique.fr (G. Saccomandi)

DNA/RNA strands [74]) show that under increasing end-to-end length these chains undergo successive events of domains unravelling. These phenomena are revealed by a (typically periodic) sequence of stress drops (see Fig. 1_b) corresponding to an increase of the contour length due to the availability of new monomers arising by the single domain unravelling (the periodicity of the diagram reveals that each drop corresponds to all-or-none single domain unravelling [67]).

To describe this behavior we model each macromolecule as a lattice of two states domains that can undergo a *hard* (folded) $\rightarrow$ *soft* (unfolded) transition under growing force. To this scope, following [19], we consider a Griffith energy minimization scheme searching for the global minima of the total (entropic plus unfolding) potential energy of the chain. Specifically, we consider identical folded domains, with the same unfolding energy Q, representing the energy dissipated in the folded-unfolded transition, and a constant number of monomers released in each transition, leading to an increase l_c of the contour length. Moreover, we neglect (see [19]) the elasticity and the dimension of the folded domains and the mixing (folded/unfolded) entropy.

Under these hypotheses one can show (see again [19] for a statistical justification based on an Ising type transition energy) that the total energy of the chain depends on the only end-to-end length L and total number n of unfolded domains. Indeed, by considering the *Worm Like Chain* (WLC) elastic energy of the unfolded fraction as proposed in [50], the total energy is given by

$$\Phi^{WLC} = \Phi_e^{WLC} + nQ, \tag{1}$$ {llll}

where

$$\Phi_e^{WLC} = \kappa \left(\frac{\lambda_r^2}{1-\lambda_r} + 2\lambda_r^2 \right) L_c \tag{2}$$

is the entropic energy of the unfolded fraction, nQ is the energy expended to unfold n domains. Here

$$\kappa = \frac{k_B T}{4p}$$

with k_B the Boltzmann constant, T the temperature, p the persistence length. Moreover we introduced the relative chain stretch

$$\lambda_r = \frac{L}{L_c} \in (0,1)$$

where

$$L_c = \hat{L}_c(n) = n l_c, \qquad n \in (n_o, n_t) \tag{3}$$ {lcc}

is the chain contour length, n_o is the virgin (reference) number of unfolded domain and n_t is the total number of hard domains in the macromolecule. Notice that the initial (undamaged) contour contour length is

$$L_c^0 = n_o l_c \tag{4} \quad \{\texttt{Lo}\}$$

and the fully unfolded (damage saturation) contour length is

$$L_c^1 = n_t l_c \tag{5} \quad \{\texttt{Lu}\}$$

so that $L_c \in (L_c^0, L_c^1)$.

In order to attain fully analytical solutions, fundamental in the following deduction of the three dimensional model, we consider the simplified expression of the WLC energy density proposed in [19] that keeps the same asymptotic behavior (as $L \to L_c$) of the WLC model proposed in [50]

$$\Phi_e = \kappa \frac{\lambda_r^2}{1-\lambda_r} L_c. \tag{6} \quad \{\texttt{Phie}\}$$

By differentiating with respect to L we get the force-stretch relation

$$f = \kappa \frac{2\lambda_r - \lambda_r^2}{(1-\lambda_r)^2}. \tag{7} \quad \{\texttt{WLC}\}$$

Of course the total energy (see (1)) is given by

$$\Phi = \Phi_e + nQ. \tag{8} \quad \{\texttt{Toten}\}$$

The same approach has been considered in polymer damage mechanics (see [18], [20] and references therein) and in the decohesion problems (see [61] and references therein). It is important to observe that the effective unfolding strategy is affected by the ability of the system of overcoming energy barriers and thus depends on the rate of deformation. Here, aimed again to a fully analytical approach, following the time scale separation proposed in [19], we consider the classical Maxwell hypothesis (see *e.g.* [5]) that the configurations of the system corresponds always to the *global* minimizers of the total energy.

One can show (see Fig. 1_a and the proof in [19]) that under this hypothesis the domains, according with the experimental observations described above, unfold following a sequence of single domain transitions that by correspond

to the condition $\Phi(L,n)-\Phi(L,n+1)=0, \quad n=0,...,n_t-1$. As a result we obtain the n dependent unfolding length

$$L^{un}=L^{un}(n)=\frac{2n+1-\sqrt{4\zeta n(n+1)+1}}{2(1-\zeta)}\,l_c, \tag{9}$$ {lthr}

where for simplicity we omit the n dependence of L_c. Here

$$\zeta=\frac{\kappa\, l_c}{Q}, \tag{10}$$

is the main non dimensional parameter of the system that measures the ratio between unfolding and elastic energy of the single hard domain. Observe that $L^{un}\in(0,L_c)$ and that L^{un} increase with n ($\frac{dL^{un}}{dn}>0$) so that the n-th branch delivers the global minimum of the energy in the interval

$$L\in(L^{un}(n-1),L^{un}(n)), \quad n\in(1,n_t-1),$$

Using (7), we get the unfolding force

$$f^{un}=f^{un}(n)=\frac{k_bT}{4L_p}\frac{2\zeta n(n+2)+1+(2\zeta n+1)\sqrt{4\zeta n(n+1)+1}}{2\zeta^2n^2}. \tag{11}$$ {fthr}

In Fig.1 we describe the typical behavior of a chain under the hypothesis that its configurations correspond to the global minima of the energy. In the figure we schematically show the decomposition of the external work into unfolding (dissipated) and elastic energy. In particular, according with the considered Maxwell hypothesis, the system follows an equilibrium branch until the elastic energy difference (between the two branches) equals the dissipation Q. Observe that the chain follows the typical sawtooth transition path observed in protein macromolecules with periodic transitions corresponding to the unfolding of single domains and the resulting entropy jump (force drop) due to the periodic unraveling of a fixed number of monomers.

Regarding the behavior of the system under unloading, we remark that an important hypothesis of the model is *unfolding irreversibility* assuming that the unfolded domains cannot refold upon unloading. More general assumptions in this direction can be considered by introducing an healing effect (see [21], [68]). As a result if the system is unloaded at a given equilibrium branch n it follows this branch until both stretch and force goes to

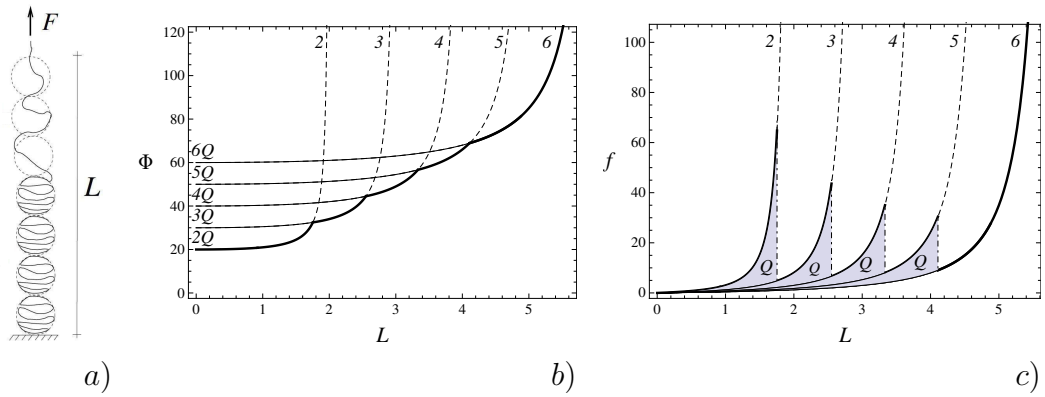


Figure 1: Unfolding behavior for a system with $n_o = 2$ and $n_t = 6$. Here we considered the parameters $Q = 10$, $\zeta = 0.1$ and $l_c = 1$. Each equilibrium path is labelled by the number n of unfolded domains. modelsoft

zero. Under reloading the system follows again the same branch and it may undergo another hard-soft transition at the same value of primary loading $L^{un} = L^{un}(n)$. Consequently, *the memory of the system is restricted to the only maximum value attained in the past by the end-to-end length* L^{max}.

3. Continuum Limit

In this section, aimed to the deduction of a continuum three-dimensional model for macromolecular materials (see *e.g.* [23]), we analyze the continuum limit of the proposed model when the discreteness can be neglected (*i.e.* $n_t \to \infty$). To get this limit we fix the *total unfolded length*, that by (3) is

$$L_c^1 = n_t l_c, \tag{12}$$ {tcl}

and consider the limit when both $l_c \to 0$ and $n_t \to \infty$. A more rigorous mathematical approach would require a discrete-continuum Γ-limit (see *e.g.* [60] and references therein where the authors deduce a continuum damage model useful in the description of peeling in biological adhesion [61]).

To this scope, we first introduce the (continuum) *damage variable*

$$\nu := \frac{n}{n_t} \in (\nu_o, 1), \tag{13}$$ {nu}

representing the unfolded fraction (here $\nu_o = n_o/n_t$ represents the unfolded fraction of the 'virgin' configuration). In the language of Continuum Mechanics ν represents a damage internal variable, with $\nu \in (\nu_o, 1)$ where $\nu = \nu_o$ represents the virgin state and $\nu = 1$ in the fully unfolded state [16, 17] (damage saturation).

As a result the elastic energy Φ^e is again given by (6) where the total contour length is using (3) given by

$$L_c = L_c(\nu) = \nu L_c^1 \in (L_c^0, L_c^1). \tag{14}$$ {Lcnu}

Notice that in our model the damage variable ν measures the change of contour length with, in particular, $L_c = L_c^0$ in the virgin configuration ($\nu = \nu_o$) and $L_c = L_c^1$ in the damage saturation configuration ($\nu = 1$). Moreover, in view of (14), the relative deformation variable depends on the continuum damage variable ν according with the following relation

$$\lambda_r = \lambda_r(L, \nu) = \frac{L}{L_c(\nu)} = \frac{L}{\nu L_c^1}. \tag{15}$$ {etac}

Similarly the total energy Φ can be expressed as

$$\Phi = \Phi(L, \nu) = \Phi_e(L, \nu) + \nu n_t Q = \kappa \frac{\lambda_r^2}{1 - \lambda_r} \nu L_c^1 + \nu n_t Q. \tag{16}$$ {Toten}

Finally observe that equilibrium equation

$$f = \partial_L \Phi_e(L, \nu) \tag{17}$$ {eeqq}

gives again the expression (7) of the equilibrium force.

An important result in the analysis of the continuum limit of the unfolding chain is that the unfolding events are characterized by a *fixed unfolding force* (stress plateau) obtained by (11) in the limit $n_t \to \infty$

$$f^{un} = \kappa \frac{2\sqrt{\zeta} + 1}{\zeta} \tag{18}$$

and a *fixed unfolding relative stretch* $\lambda_r = \lambda_r^{un}$, with

$$\lambda_r^{un} = \frac{1}{\sqrt{\zeta} + 1}, \tag{19}$$ {luuu}

continuous analog of (9). This corresponds to an unfolding length

$$L^{un} = \nu \frac{L_c^1}{\sqrt{\zeta}+1} = \nu \lambda_r^{un} L_c^1.$$

As a result the behavior of the chain is assigned by the parameters that can be deduced by the single β sheet, L_p, l_c and ζ (or analogously the unfolding stretch λ_r^{un}), and by the only initial number of unfolded elements n_o and the total number of elements n_t (or analogously L_c^0 and L_c^1). It is important to remark that the unfolding relative stretch and force depend on the barrier Q that, as observed in [19] and references therein may depend on the rate of deformation. In the following we consider the limit of slow stretching rates and a rate-independent value of Q and ζ.

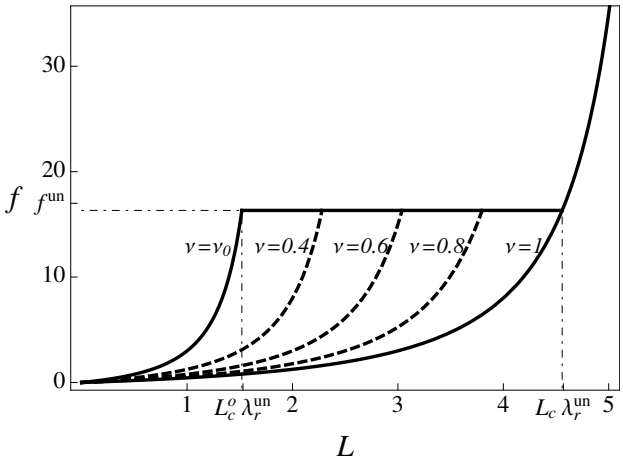


Figure 2: Unfolding behavior in a continuum system with the same parameters of Fig.1. Each equilibrium path is labelled by the damage ν. modelcont

In particular the value of the unfolding length is a function of the internal damage variable ν:

$$L^{un} = L^{un}(\nu) = \lambda_r^{un} L_c(\nu) = \nu \lambda_r^{un} L_c^1 \in (\lambda_r^{un} L_c^0, \lambda_r^{un} L_c^1). \qquad (20) \quad \{\texttt{LU}\}$$

The behavior of the system is illustrated in Fig.2. If we begin loading the chain the damage begins at $L = L^{un}(L_c^0) = \lambda_r^{un} L_c^0$ (point A in the figure) that represents the virgin elastic threshold and for $L^{max} \leq L^{un}(L_c^0)$ the behavior is purely elastic. If the end-to-end length is increased further, the chain unfolds

following the stress plateaux (A-B-C in the figure) $f = f^{un}$. The damage saturation is attained at $L = \lambda_r^{un} L_c^1$ (point C) so that for $L^{max} \geq \lambda_r^{un} L_c^1$ the behavior is again elastic with a fixed damage $\nu = 1$ (curve O-C-D). If we unload before damage saturation is attained (*e.g.* point B in the figure) the system follows an equilibrium branch at fixed damage ν (curve B-O). Similarly if we reload the system follows the same branch until $L = L^{max}$ (B) when the unfolding fraction ν starts increasing.

Notice that, as in the discrete case considered in the previous section, the memory of the system is restricted to L^{max}. In particular

$$\nu = \bar{\nu}(L^{max}) = \frac{L^{max}}{\lambda_r^{un} L_c^1} = \frac{L^{max}}{L_c^1}(\sqrt{\zeta} + 1) \qquad L^{max} \in (\lambda_r^{un} L_c^0, \lambda_r^{un} L_c^1). \tag{21}$$ {nuL}

3.1. Thermodynamical consistence of the continuum damage model

We observe that the deduced model can be inscribed in the framework of Thermodynamics with internal state variables [15] in the special simple setting of *isothermal processes*. Indeed the state of the continuum chain can be assigned by a single 'external variable' L and a single 'internal variable' ν. Following [15] we may then introduce the rate of entropy production

$$\frac{\gamma}{T} = \dot{S}(L, \nu) + \frac{f\dot{L}}{T},$$

where

$$\dot{S} = -\frac{\dot{\Phi}_e}{T},$$

is the entropy of the chain. The classical (Clausius-Duhem type) dissipation inequality [15] requires that

$$\frac{\gamma}{T} = \frac{1}{T}\left[(-\partial_L \Phi_e(L, \nu) + f)\,\dot{L} + g\dot{\nu}\right] \geq 0. \tag{22}$$ {dis}

where

$$g = g(L, \nu) = -\partial_\nu \Phi_e(L, \nu) = \kappa \frac{\lambda_r^2}{(1 - \lambda_r)^2} L_c^1 > 0 \tag{23}$$ {ddff}

is the generalized force working for damage growth.

Moreover, using the equilibrium equation (17), we obtain the reduced dissipation (variational) inequality

$$\gamma = g\dot{\nu} \geq 0 \tag{24}$$ {rCD}

that using (23) ensures that the Clausius Duhem inequality is respected if an only if our irreversibility hypothesis

$$\dot{\nu} \geq 0$$

is fulfilled.

To show that our model can be inscribed in the classical damage mechanics, we observe that the activation of damage can be equivalently assigned by the three simple conditions

$$h_L(L) = L - L^{un} = 0, \qquad h_f(f) = f - f^{un} = 0, \qquad h_{\lambda_r}(\lambda_r) = \lambda_r - \lambda_r^{un} = 0, \tag{25}$$ {thresh}

defining in particular the present elastic domain as a function of ν.

Thus, since when damage is active we have

$$L = L^{max} = L^{un}(\nu), \tag{26}$$

using (20) we obtain the flow rule

$$\dot{\nu} = \dot{\nu}(L, \dot{L}, \nu) = \begin{cases} 0 & \text{if} \quad L < L^{un}, & \text{elastic regime,} \\ 0 & \text{if} \quad L = L^{un}, \dot{L} \leq 0, & \text{elastic unloading,} \\ \dfrac{\dot{L}}{\lambda_r^{un} L_c^1}, & \text{if} \quad L = L^{un}, \dot{L} > 0, & \text{damage regime.} \end{cases}$$

To evaluate the dissipation potential D we observe that when damage is active after easy computations we have

$$g = g(L^{un}(\nu), \nu) = n_t Q$$

so that

$$D = D(\dot{\nu}) = n_t Q\, \dot{\nu}.$$

In particular, we obtain a constant dissipation rate and a rate independent dissipation behavior (the potential is a homogeneous function of degree one).

Finally, it is interesting to observe, both from a theoretical and numerical point of view, that the unfolding behavior of the system can be obtained through a variational approach, considering a Griffith-type minimization scheme for the total (elastic plus unfolding) potential energy

$$G(L, \nu) = \Phi(L, \nu) - fL.$$

Indeed if we consider the constrained minimization problem

$$\min_{\nu \geq \bar{\nu}, L} G(L, \bar{\nu}),$$

where $\bar{\nu}$ is the present value of damage, the damage evolution equations result as classical Kuhn-Tucker minimization conditions (see *e.g.* [3]) for the Lagrangian function $\mathcal{L} = G(L, \bar{\nu}) + \mu\,(\bar{\nu} - \nu)$:

$$\begin{cases} \partial_L \mathcal{L} = L_c^1 \partial_L \varphi_e - f = 0, \\ \partial_\nu \mathcal{L} = nQ - g - \mu = 0, \\ \nu \geq \bar{\nu}, \\ \mu \geq 0, \\ \mu(\nu - \bar{\nu}) = 0 \Rightarrow (q - g)(\nu - \bar{\nu}) = 0. \end{cases} \tag{27}$$ {KT}

By these conditions we deduce the equilibrium equation

$$f = \partial_L \Phi_e,$$

the consistency condition

$$(n_t Q - g)(\bar{\nu} - \nu) = 0,$$

assuring that the unfolding can happen only on the thresholds defined in (25). Moreover, since $\mu \geq 0$, we obtain the admissibility conditions

$$g \leq n_t Q \Rightarrow f \leq f^{un}, L \leq L^{un}.$$

Remark 1. We may observe that since the energy is positive semidefinite these conditions are also sufficient to attain the global minimum of the total energy G [3], representing the *unique* solution due to the convexity of the energy function.

Remark 2. It is easy to verify that the conditions (27) correspond to the classical condition of *maximal dissipation* adopted in non equilibrium Thermodynamics [86]. Indeed, if we consider the incremental variational problem for (24)

$$\max_{g-n_tQ\leq 0} \gamma = \max_{g-n_tQ\leq 0} g\dot{\nu}$$

we obtaion the Kuhn Tucker condition $(g - n_tQ)\dot{\nu} = 0$.

3.2. Chain elastic and residual stretches

In the spirit of deducing a continuum three dimensional model, and with the aim of interpreting the experimentally observed macroscopical residual stretches as an effect of the unfolding, we here introduce the notion of elastic, plastic and total stretch for the chain.

As discussed above, the contour length of the chain, due to the new available monomers resulting from crystals unfolding events (see the schematic representation in Fig.3), changes with the maximum attained elongation (14)

$$L_c = \nu L_c^1 = \nu n_t l_c. \tag{28}$$ {Lcb}

Based on classical Statistical Mechanics results [71] the natural length of the chain depends on the present number of unfolded hard crystals through the relation

$$L_p = L_p(\nu) = \sqrt{\bar{n}}b = \sqrt{\nu\bar{n}_t}b, \tag{29}$$ {llpp}

giving the natural (zero force) length of the chain once the number of unfolded Kuhn segments

$$\bar{n} = n_k n$$

and their length b is known. Here $n_k = l_c/b$ is the number of Kuhn segments inside each unfolded domain and

$$\bar{n}_t = \frac{l_c}{b} n_t = n_k n_t \tag{30}$$ {nnt}

is the total number of Kuhn segments. In particular we denote by

$$L_o = \sqrt{\nu_o \bar{n}_t}b. \tag{31}$$ {Lo}

We then define the following stretch measures

$$\begin{cases} \lambda = \dfrac{L}{L_o}, & (total)\ \ stretch, \\ \lambda_e = \dfrac{L}{L_p(\nu)}, & elastic\ \ stretch, \\ \lambda_p = \dfrac{L_p(\nu)}{L_o}, & permanent\ \ stretch \end{cases} \tag{32} \quad \{\texttt{str}\}$$

verifying the classical deformation composition (see Fig.3)$\lambda = \lambda_e \lambda_p$. Moreover it is easy to verify that

$$\lambda = \nu \sqrt{\frac{\bar{n}_t}{\nu_o}}\ \lambda_r, \quad \lambda_e = \sqrt{\nu \bar{n}_t}\, \lambda_r, \quad \lambda_p(\nu) = \sqrt{\frac{\nu}{\nu_o}}. \tag{33} \quad \{\texttt{abc}\}$$

We may then introduce the energy density

$$\phi_e = \phi_e(\lambda, \nu) := \frac{\Phi_e(\lambda L_o, \nu)}{L_o}$$

that using (17) and $(32)_1$ gives

$$f = \partial_\lambda \phi_e(\lambda, \nu). \tag{34}$$

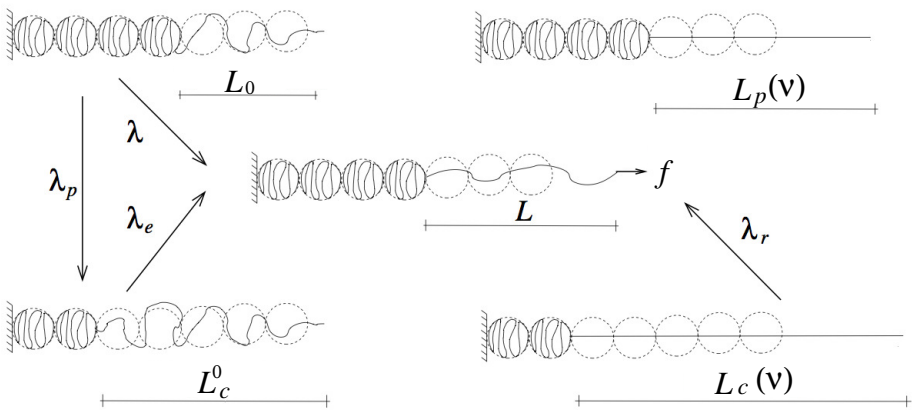
To complete the "continuum" extension we have to rephrase the damage evolution law (21) in terms of the stretch λ. Since according with $(32)_1$ the maximum attained stretch λ^{max} corresponds to L^{max}, using (21), (12) and (31) we obtain

$$\nu = \sqrt{\frac{\nu_o}{\bar{n}_t}}\ \frac{\lambda^{max}}{\lambda_r^{un}}, \qquad \lambda \in (\lambda_o, \lambda_1). \tag{35} \quad \{\texttt{nunu}\}$$

Here

$$\lambda_o = \sqrt{\nu_o \bar{n}_t}\lambda_r^{un}, \qquad \lambda_1 = \sqrt{\frac{\bar{n}_t}{\nu_o}}\lambda_r^{un} \tag{36} \quad \{\texttt{thress}\}$$

are the stretches corresponding to damage initiation (see (31)) and damage saturation (see (5)), respectively.



lu

Figure 3: Scheme of the elastic, plastic, total and relative stretches. {scc}

4. Three dimensional unfolding networks: macroscopic energy density

In this section we consider the second scale passage, deducing a three dimensional non-linear damage *macroscopic* limit based on the energy minimization results of the single macromolecule obtained in the previous section. The aim of this model is to predict the dissipative and softening behavior of continuum macromolecular bodies with unfolding chains.

Let $\boldsymbol{f}$ be the deformation function for a continuous body and let $\boldsymbol{B}$ be the left Cauchy-Green strain tensor

$$\boldsymbol{B} = \nabla \boldsymbol{f} (\nabla \boldsymbol{f})^T = \lambda_1^2 \boldsymbol{e}_1 \otimes \boldsymbol{e}_1 + \lambda_2^2 \boldsymbol{e}_2 \otimes \boldsymbol{e}_2 + \lambda_3^2 \boldsymbol{e}_3 \otimes \boldsymbol{e}_3, \qquad (37) \quad \{\texttt{CG}\}$$

where λ_i and $\boldsymbol{e}_i$, $i = 1, 2, 3$, are the principal stretches and the principal unit vectors, respectively. In the following, as usual for polymeric materials and many biological materials, we assume incompressibility, so that

$$\det \boldsymbol{B} = \lambda_1^2 \lambda_2^2 \lambda_3^2 = 1.$$

To obtain the constitutive behavior of materials constituted by unfolding macromolecules we first need to connect the macroscopic stretches to the chains elongations. We here deduce this relations based on the classical

assumption of *affine deformations*, assuming the chains elongations coincide with the macroscopic stretches (see *e.g.* [87] for an analysis of the limits of this simplifications).

Based on this simple approach, we also show that an analysis of the variable configuration of the chains due to macromolecule unfolding delivers a natural way of deducing the presence of permanent stretches observed in the experimental behavior of biological materials with unfolding chains (see the schematic representation in Fig.3).

4.1. Isotropic damage energy: 8-chain model

To obtain the macroscopic constitutive law of the macromolecular continuum body, a general approach would require the analysis of a continuum distribution of chains as in the full network model (see Wu and Van der Giessen [84] and [51]). In this case the energy density depends on the orientation and distribution of the chains. The resulting model can be numerically heavy (see [2] for an efficient numerical approach of the resulting model).

Here we follow the Arruda-Boyce 8-chain approach [1] and deduce an isotropic damage model. Let then N be the number of chains per unit volume. In the case of the well known Arruda Boyce eight chains model, the authors show that considering a cubic unit chains cell with faces parallel to the stretch eigenvectors $\boldsymbol{e}_1, \boldsymbol{e}_2, \boldsymbol{e}_3$ (see (37)), with the N chains distributed along the eight diagonals connecting the vertexes to the cell center, is energetically equivalent to consider all N chains aligned in the direction

$$\boldsymbol{m} = \frac{1}{\sqrt{3}}(\boldsymbol{e}_1 + \boldsymbol{e}_2 + \boldsymbol{e}_3)$$

with all chains characterized by the same stretch

$$\lambda = \sqrt{\frac{I}{3}} \qquad (38) \quad \{\texttt{princ}\}$$

where $I = \text{tr } \boldsymbol{B}$.

The main idea of the 8-chain approach is clarified by the observation that the first invariant I, according with a simple result by Kearsley [41], is equal to "three times the square of the stretch ratio of an infinitesimal line element averaged over all possible orientations". An important consequence of this observation is that the 8-chain approximation let us deduce the evolution of both damage and residual stretch only in an "averaged sense". As a result, we

here obtain an isotropic damage model and an isotropic hardening plasticity condition with all chains undergoing the same damage and the same residual stretch.

More realistic results in this perspective requires the use of anisotropic multiscale approaches such as the three chains model or the full network approach [51, 2] that will be the subject of our future work.

In particular under this simplifying assumption since all chains undergo the same elongation, both damage and plastic effects are assumed to be isotropic. As a result we consider, using $(32)_3$ a spherical plastic deformation tensor

$$\boldsymbol{F}_p = \sqrt{\frac{\nu}{\nu_o}}\boldsymbol{I},$$

with a simple form of the multiplicative decomposition

$$\boldsymbol{F} = \boldsymbol{F}_e\boldsymbol{F}_p = \sqrt{\frac{\nu}{\nu_o}}\boldsymbol{F}_e. \tag{39}$$ {FF}

where we assume elastic incompressibility ($\det \boldsymbol{F}_e = 1$).

To determine the macroscopic energy we may relate, based on (38) the chain relative stretch to the first invariant I. Indeed, using $(33)_1$ we have that

$$\lambda_r = \frac{\lambda}{\lambda_c} = \sqrt{\frac{I}{I_c}} \tag{40}$$ {dom}

where, based on $(33)_1$, we introduced the critical value of the stretch $\lambda_c = \nu\sqrt{\frac{\bar{n}_t}{\nu_o}}$ and of the first invariant

$$I_c = 3\lambda_c^2 = 3\nu^2\frac{\bar{n}_t}{\nu_o}, \qquad I_c \in (I_c^o, I_c^1), \tag{41}$$ {icic}

such that the representative chain in the 8-chain model reaches its (damage dependent) contour length ($\lambda_r = 1$). This microstructure resulting limit threshold for I takes the same role of the limit threshold of the classical Gent model in rubber elasticity [36]. Here I_c can be seen as a fair (and natural) measure of the average contour length of the chains composing the network. In (41)

$$I_c^o = 3\nu_o\bar{n}_t \quad \text{and} \quad I_c^1 = 3\frac{\bar{n}_t}{\nu_o}$$

represent the virgin and damage saturations (contour length) thresholds, respectively. Moreover, using (35), since by (38) $I^{max} = 3(\lambda^{max})^2$, we obtain

$$I_c = \frac{I^{max}}{(\lambda_r^{un})^2}, \qquad I^{max} \in (I^o, I^1), \tag{42}$$ {IcIc}

with λ_r^{un} the material parameter in (19) and

$$I^o = 3\nu_o \bar{n}_t (\lambda_r^{un})^2 \quad \text{and} \quad I^1 = 3\frac{\bar{n}_t}{\nu_o}(\lambda_r^{un})^2$$

the virgin and damage saturations invariant thresholds, respectively.

Based on this analysis, it is now possible to deduce the macroscopic energy density starting from the energy of the chain (16). Indeed, based on the classical additivity assumption, the energy density per unity volume of a network with N chains per unit volume is given by

$$\varphi = \varphi_e + \nu q \tag{43}$$ {contte}

where

$$\varphi_e = N\Phi_e(L, \nu) = NL_o\phi_e(\lambda, \nu)$$

and

$$q = Nn_tQ$$

is the total dissipation for the full unfolding of the N chains in the cell.

Using (6) and (33) we obtain

$$\varphi_e = N\kappa\frac{\lambda_r^2}{1-\lambda_r}\nu L_c^1 - c, \tag{44}$$ {fifi}

where c is the usual normalizing constant such that $\varphi_e = 0$ in the reference configuration. As a result, since $L_c^1 = \bar{n}_t b$, we obtain, using (41)

$$\varphi_e = \frac{\mu_o}{2}\frac{\sqrt{\frac{I_c^o}{I_c}}}{1-\sqrt{\frac{I}{I_c}}}I - c, \tag{45}$$ {contphi}

where

$$\mu_o = \frac{2}{3}\kappa Nb = \frac{Nb}{6p}k_BT$$

is the (virgin) infinitesimal shear modulus.

Under the assumption of elastic incompressibility we obtain the kinematic constraint

$$\det \boldsymbol{F} = \left(\frac{\nu}{\nu_o}\right)^{\frac{3}{2}} = \left(\frac{I_c}{I_c^o}\right)^{\frac{3}{4}} \qquad (46) \quad \{\texttt{kk}\}$$

showing the volume growth effect induced by the increase of chain length (29) due to the new available monomers related to unfolding. As a result the macroscopic constitutive law that, using (43) and (45), assigns the Cauchy stress tensor

$$\boldsymbol{T} = -p\boldsymbol{I} + (\det \boldsymbol{F})^{-1}\partial_{\boldsymbol{F}}\varphi(I, I_c)\boldsymbol{F}^T = -p\boldsymbol{I} + \aleph(I, I_c)\boldsymbol{B} \qquad (47) \quad \{\texttt{equilb}\}$$

where we used (39) and

$$\aleph(I, I_c) = \mu_o \frac{1 - \frac{1}{2}\sqrt{\frac{I}{I_c}}}{\left(1 - \sqrt{\frac{I}{I_c}}\right)^2} \left(\frac{I_c^o}{I_c}\right)^{\frac{5}{4}},$$

where I_c is given in (42), whereas p is the pressure arising from the kinematic constrain (46).

Also we observe that on the primary loading path $I = I^{max}$, using (42) we have a constant value of $\aleph$:

$$\bar{\aleph}(I) = \aleph(I^{max}, I_c) = \mu_o (\lambda_r^{un})^{\frac{5}{2}} \frac{2 - \lambda_r^{un}}{2(1 - \lambda_r^{un})^2} \left(\frac{I_c^o}{I}\right)^{5/4}.$$

As a result we have that the Cauchy stress is given by

$$\boldsymbol{T} = \begin{cases} -p\boldsymbol{I} + \aleph(I, I_c^o)\boldsymbol{B} & \text{if} \quad I^{max} \le I_o & \text{virgin elastic regime,} \\ -p\boldsymbol{I} + \aleph(I, \frac{I^{max}}{(\lambda_r^{un})^2})\boldsymbol{B} & \text{if} \quad I_o < I^{max} < I_1, \dot{I}^{max} = 0 & \text{fixed damage regime,} \\ -p\boldsymbol{I} + \bar{\aleph}(I) & \text{if} \quad I_o < I^{max} < I_1, \dot{I}^{max} > 0 & \text{growing damage regime,} \\ -p\boldsymbol{I} + \aleph(I, I_c^1)\boldsymbol{B} & \text{if} \quad I^{max} \ge I_1 & \text{damage saturation regime.} \end{cases}$$

To verify the thermodynamical consistence of the model we observe that the Clausius-Duhem inequality requires the positivity of the rate of entropy density production

$$\frac{\gamma}{T} = -\frac{\dot{\varphi}_e}{T} + \frac{\boldsymbol{T}\boldsymbol{F}^{-T} \cdot \dot{\boldsymbol{F}}}{T} \ge 0.$$

Notice that in our entropic elasticity model $-\frac{\varphi_e}{T}$ is the entropy density function. Thus we obtain in view of (45)

$$(-\partial_{\boldsymbol{F}}\varphi_e + \boldsymbol{T}\boldsymbol{F}^{-T}) \cdot \dot{\boldsymbol{F}} + g\dot{\nu} \geq 0$$

where

$$g = g(I^e, \nu) = \mu_o \frac{\sqrt{\frac{I^e}{I_c^e}}}{\left(1 - \sqrt{\frac{I^e}{I_c^e}}\right)^2} \frac{I_e}{4\nu}$$

that, using (**??**) and (**??**) can be rewritten in term of I as

$$g = g(I, \nu) = \mu_o \frac{\sqrt{\frac{I}{I_c}}}{\left(1 - \sqrt{\frac{I}{I_c}}\right)^2} \frac{\nu_o I}{4\nu^2}.$$

Using (47) with the constraint $\boldsymbol{F}^{-T} \cdot \dot{\boldsymbol{F}} = 0$, due to the incompressibility assumption, we obtain the reduced dissipation inequality (CORREGGI)

$$g\dot{\nu} = \mu_o \frac{\sqrt{\frac{I}{I_c}}}{8\left(1 - \sqrt{\frac{I}{I_c}}\right)^2} I \frac{\dot{I}^{max}}{I^{max}} \geq 0.$$

Moreover we may observe that $g(., I^{max})$ grows we have that the maximum dissipation is attained when $I = I^{max}$ when the dissipation rate equals the dissipation potential

$$D = g(I^{max}, I^{max})\dot{\nu} = \frac{\mu\theta}{4(\theta - 1)^2}(I^{max} - 3)\,\frac{\dot{I}^{max}}{I^{max}}.$$

Finally we observe that since $\frac{\partial \varphi^e(I^e,\nu)}{\partial I^e} > 0$ and $\frac{\partial^2 \varphi^e(I^e,\nu)}{\partial^2 I^e} > 0$, the elastic energy is a polyconvex function of the elastic strain $\boldsymbol{F}^e$ for all $\nu \geq \nu_o$ [82].

5. Numerical examples and comparisons with experiments

We consider the two simple cases of unitxial extension and biaxial extension.

5.0.1. Uniaxial extension

Consider first the simple case of uniaxial extension schematized in Fig.4_a with

$$\boldsymbol{B} = \begin{bmatrix} \lambda^2 & 0 & 0 \\ 0 & \left(\frac{I_c}{I_c^o}\right)^{\frac{3}{4}} \lambda^{-1} & 0 \\ 0 & 0 & \left(\frac{I_c}{I_c^o}\right)^{\frac{3}{4}} \lambda^{-1} \end{bmatrix},$$

respecting the kinematic constraint (46) and

$$I = \lambda^2 + 2\left(\frac{I_c}{I_c^o}\right)^{\frac{3}{4}} \frac{1}{\lambda}.$$

By imposing $\boldsymbol{T}_{22} = \boldsymbol{T}_{33} = 0$, we determine the pressure

$$p = \aleph \left(\frac{I_c}{I_c^o}\right)^{\frac{3}{4}} \frac{1}{\lambda},$$

so that we obtain the stress strain relation

$$t = \boldsymbol{T}_{11}(\lambda) = \aleph \left(\lambda^2 - \left(\frac{I_c}{I_c^o}\right)^{\frac{3}{4}} \frac{1}{\lambda}\right)$$

the corresponding component of the engineering (Piola) stress $\boldsymbol{S} = \boldsymbol{T}\,\boldsymbol{F}^*$ (with $\boldsymbol{F}^* = \det\boldsymbol{F}\,\boldsymbol{F}^{-T}$) is given by

$$s = \boldsymbol{S}_{11}(\lambda) = \aleph \left(\left(\frac{I_c}{I_c^o}\right)^{\frac{3}{4}} \lambda - \left(\frac{I_c}{I_c^o}\right)^{\frac{3}{8}} \frac{1}{\lambda^2}\right).$$

5.0.2. Biaxial extension

Consider now the case of biaxial extension schematized in Fig.5_b Let

$$\boldsymbol{F}^e = \begin{bmatrix} \lambda_e & 0 & 0 \\ 0 & \lambda_e & 0 \\ 0 & 0 & \lambda_e^{-2} \end{bmatrix}.$$

Thus we have

$$\boldsymbol{F} = \begin{bmatrix} \lambda & 0 & 0 \\ 0 & \lambda & 0 \\ 0 & 0 & \left(\frac{\nu}{\nu_o}\right)^{\frac{3}{2}} \lambda^{-2} \end{bmatrix}$$

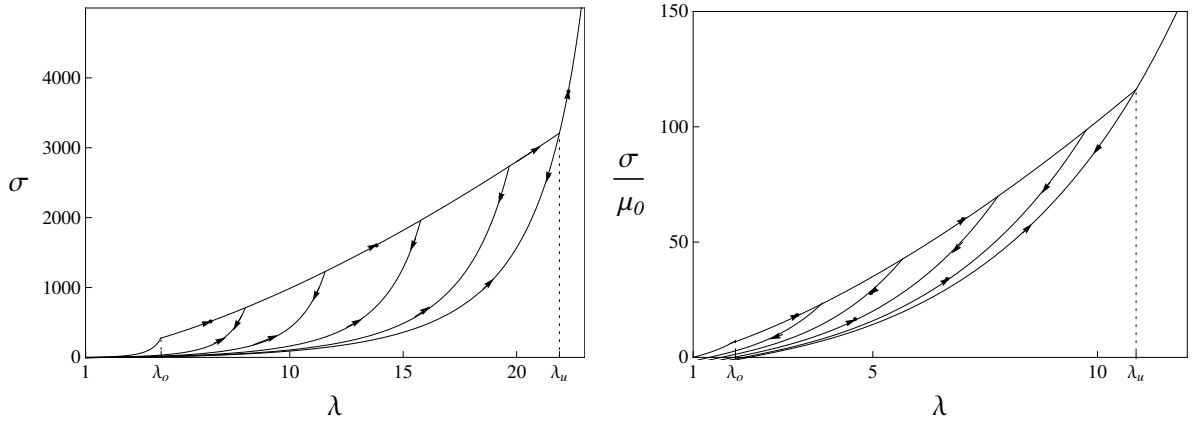


Figure 4: ⌈SE

and

$$I = 2\lambda^2 + \left(\frac{\nu}{\nu_o}\right)^3 \frac{1}{\lambda^4},$$

where $\lambda = \sqrt{\frac{\nu}{\nu_o}}\lambda_e$.

By imposing $\boldsymbol{T}_{33} = 0$, we determine the pressure

$$p = \aleph \left(\frac{\nu}{\nu_o}\right)^{\frac{5}{2}} \frac{1}{\lambda^4},$$

so that we obtain the stress strain relation

$$\sigma = \boldsymbol{T}_{11}(\lambda) = \aleph \left(\sqrt{\frac{\nu_o}{\nu}}\lambda^2 - \left(\frac{\nu}{\nu_o}\right)^{\frac{5}{2}} \frac{1}{\lambda^4}\right)$$

the corresponding component of the engineering (Piola) stress $\boldsymbol{S} = \boldsymbol{T}\boldsymbol{F}^{-T}$ is given by

$$s = \boldsymbol{S}_{11}(\lambda) = \aleph \left(\sqrt{\frac{\nu_o}{\nu}}\lambda - \frac{\nu}{\nu_o}\frac{1}{\lambda^2}\right).$$

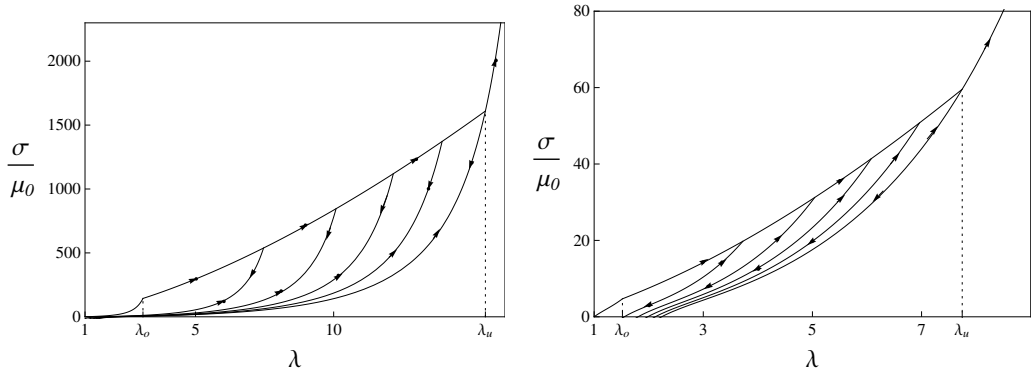


Figure 5: ⌈BE

5.0.3. Simple shear

Consider finally the case of simple shear schematized in Fig.6$_b$ Let

$$\boldsymbol{F}^e = \begin{bmatrix} 1 & k_e & 0 \\ 0 & 1 & 0 \\ 0 & 0 & 1 \end{bmatrix},$$

where k_e is the shear deformation. Thus we have

$$\boldsymbol{F} = \begin{bmatrix} \sqrt{\frac{\nu}{\nu_o}} & k & 0 \\ 0 & \sqrt{\frac{\nu}{\nu_o}} & 0 \\ 0 & 0 & \sqrt{\frac{\nu}{\nu_o}} \end{bmatrix}.$$

Thus we have

$$I = 3\frac{\nu}{\nu_o} + k^2,$$

where $k = \sqrt{\frac{\nu}{\nu_o}} k_e$.

Thus we obtain the stress strain relation

$$\tau = \boldsymbol{T}_{12}(k) = \aleph k$$

the corresponding component of the engineering (Piola) stress $\boldsymbol{S} = \boldsymbol{T}\boldsymbol{F}^{-T}$ is given by

$$t = \boldsymbol{S}_{11}(\lambda) = \aleph k_e = \aleph\sqrt{\frac{\nu_o}{\nu}} k.$$

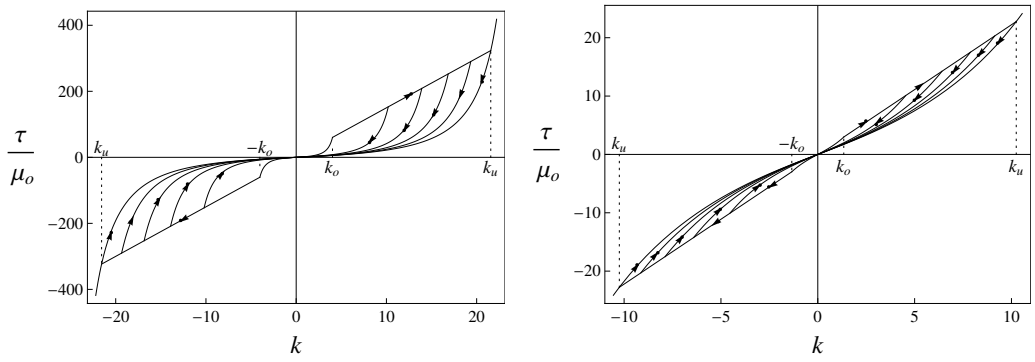


Figure 6: ⌈SS

6. Conclusions

Acknowledgments. The work of D.D. and G.P. has been supported by Progetto di ricerca industriale-Regione Puglia, Modelli innovativi per sistemi meccatronici and PRIN 2010-11: Dinamica, stabilità e controllo di strutture flessibili (Dynamics, stability and control of slender structures). G.S. is grateful to the Istituto Nazionale di Alta Matematica (Italy) and PRIN 2009 Matematica e meccanica dei sistemi biologici e dei tessuti molli for financial support.

7. Appendix: List of symbols

L	current chain length
f	force acting on the chain ends
L_c^1	totally unfolded contour length
L_c^0	initial (virgin) unfolded contour length
n_t	total number of hard domains
n_o	initial v of hard domains
n	current number of hard domains
l_c	contour length of the single hard domain
ν	damage (internal) variable
ν_o	initial (virgin) fraction of unfolded domains
ν	damage (internal) variable
ν	damage (internal) variable
ν	damage (internal) variable
ν	damage (internal) variable
ν	damage (internal) variable
ν	damage (internal) variable
ν	damage (internal) variable

[1] E.M. Arruda, M.C. Boyce, 1993, A three-dimensional model for the large stretch behavior of rubber elastic materials,, J. Mech. Phys. Solids, 41(2), pp. 389–412.

[2] P. Bažant, B. H. Oh, 1986, Efficient Numerical Integration on the Surface of a Sphere, ZAMM, 66(1), pp. 37–49. Doi: 10.1002/zamm.19860660108

[3] M.S. Bazaraa,H. D. Sherali, C. M. Shretty (2006). Nonlinear programming. Theory and Algorithms Third Edition. J. Wiley

[4] I. Benichou and S. Givli 2011 The hidden ingenuity in titin structure, *Appl. Phys. Lett.*, **98**, 091904. (doi:http://link.aip.org/link/doi/10.1063/1.3558901)

[5] G. Bertotti *Hysteresis in magnetism*, Academic Press, Boston (1998)

[6] R.B. Best, S.B. Fowler, J.L. Toca Herrera, A Steward, E. Paci and J. Clarke 2003, Mechanical Unfolding of a Titin Ig Domain: Structure of Transition State Revealed by Combining Atomic Force Microscopy,

Protein Engineering and Molecular Dynamics Simulations, *J. Mol. Biol.*, **330**, 867-877. (doi:10.1016/S0022-2836(03)00618-1)

[7] O. V. Borisov and A. Halperin 1996, On the elasticity of polysoaps: The effects of secondary structure, *Appl. Phys. Lett.*, **34**, 657. (doi:10.1209/epl/i1996-00511-0)

[8] O. V. Borisov and A. Halperin 1997 On the extension of polysoaps: The Gaussian approximation, *Macromolecular Symposia*, **113**, 11–17. (doi:10.1002/masy.19971130104)

[9] D.J. Brockwell, E. Paci, R.C. Zinober, G.S. Beddard, P.D. Olmsted, D.A. Smith, R.N. Perham, S.E. Radford 1997 Pulling geometry defines the mechanical resistance of a beta-sheet protein., *Nat Struct Biol*, **10** 731-737. (doi:0.1038/nsb968)

[10] A.E.X. Brown, R.I. Litvinov, D.E. Discher, J.W. Weisel, (2007). Forced Unfolding of Coiled-Coils in Fibrinogen by Single-Molecule AFM, *Biophys. J.*, **92**, L39–L41. (doi:10.1529/biophysj.106.101261)

[11] J.D. Bryngelson, J.N. Onuchic, N.D. Socci, P.G. Wolynes 2004 Funnels, pathways, and the energy landscape of protein folding: A synthesis, *Proteins: Structure, Function, and Bioinformatics*, **21**, 167–195. (doi:10.1002/prot.340210302)

[12] M.J. Buehler, Y.C. Yung 2009, Deformation and failure of protein materials in physiologically extreme conditions and disease, *Nat. Mater.*, **8**, 175–188. (doi:10.1038/nmat2387)

[13] A. Buhot, A. Halperin 2000, Extension of Rod-Coil Multiblock Copolymers and the Effect of the Helix-Coil Transition, *Physical Review Letters*, **84**, 2160. (10.1103/PhysRevLett.84.2160)

[14] A. Buhot, A. Halperin 2002, Extension Behavior of Helicogenic Polypeptides, *Macromol.*, **35**, 3238–52. (doi: 10.1021/ma011631w)

[15] B.D. Coleman and M.E. Gurtin 1967, Thermodynamics with Internal State Variables, *J. Chem. Phys.*, **47**, 597–613 .

[16] D. D'ambrosio, D. De Tommasi, D. Ferri, G. Puglisi 2008, A phenomenological model for healing and hysteresis in rubber-like materials *Int. J. Engi. Sci.*, **46**, 293. (doi:10.1016/j.ijengsci.2007.12.002)

[17] A. DeSimone, J.J, Marigo, L. Teresi 2001, A damage mechanics approach to stress softening and its application to rubber, *Eur. J. Mech. A/Solids*, **20**, 873. (http://dx.doi.org/10.1016/S0997-7538(01)01171-8)

[18] D. De Tommasi, G. Puglisi (2007). Mullins effect for a cylinder subjected to combined extension and torsion Journal of Elasticity, 86 (1), pp. 85-99.

[19] D. De Tommasi, N. Millardi, G. Puglisi, G. Saccomandi, 2013, An energetic model for macromolecules unfolding in stretching experiments. *J R Soc Interface.* , **10**, 20130651. (10.1098/rsif.2013.0651)

[20] De Tommasi D., Marzano S., Puglisi G., Saccomandi G. (2010). Localization and stability in damageable amorphous solids. *Cont. Mech. Therm.*, 22 (1), 47.-62.

[21] De Tommasi D., Marzano S., Puglisi G., Zurlo, G. (2009). Damage and healing effects in rubber-like balloons. *Int. J. Sol. Struct.*, 46 (22-23), 3999-.4005.

[22] D. De Tommasi, G. Puglisi, G. Saccomandi 2008, Localized versus Diffuse Damage in Amorphous Materials, *Physical Review Letters*, **100**, 085502. (10.1103/PhysRevLett.100.085502)

[23] D. De Tommasi, G. Puglisi, G. Saccomandi 2010, Damage, Self-Healing, and Hysteresis in Spider Silks, *Biophys. J.*, **98**, 1941-1948. (doi:http://dx.doi.org/10.1016/j.bpj.2010.01.021)

[24] D. De Tommasi, G. Puglisi, G. Saccomandi 2006, A micromechanics-based model for the Mullins effect, *J. Rheology*, **50**, 495. (doi:http://dx.doi.org/10.1122/1.2206706)

[25] H. Dietz, F. Berkemeier, M. Bertz, and M. Rief, Anisotropic deformation response of single protein molecules, *Proc. Nat. Acad. Sci.*, **103**, 12724-12728.(doi:10.1073/pnas.0602995103)

[26] A.V. Dobrynin and J.Y. Carrillo 2011, Universality in Nonlinear Elasticity of Biological and Polymeric Networks and Gels, *Macromol.*, **44**, 140–146. (doi: 10.1021/ma102154u)

[27] A. Dorfmann, R. W. Ogden 2003, A pseudo-elastic model for loading, partial unloading and reloading of particle-reinforced rubber, *Int. J. Sol. Struct.*, **40**, 2699–2714. (doi:http://dx.doi.org/10.1016/S0020-7683(03)00089-1)

[28] N. Duff, N.H. Duong, D.J. Lacks 2006, Stretching the Immunoglobulin 27 Domain of the Titin Protein: The Dynamic Energy Landscape, *Biophys. J.*, **91**, 3446–3455. (http://dx.doi.org/10.1529/biophysj.105.074278)

[29] I. Ekeland, R. Temam (1976), Convex Analysis and Variational ProblemsFront Cover Elsevier, 1976

[30] E. Evans, K. Ritchie 1997, Dynamic strength of molecular adhesion bonds, *Biophys. J.*, **72**, 1541–1555. (doi:http://dx.doi.org/10.1016/S0006-3495(97)78802-7)

[31] E. Evans, K. Ritchie 1999, Strength of a Weak Bond Connecting Flexible Polymer Chains, *Biophys. J.*, **76**, 2439–2447. (doi:

[32] A.R. Fersht, V. Daggett, Protein folding and unfolding at atomic resolution 2002, *Cell*, **108**, 573-82. (doi:http://dx.doi.org/10.1016/S0092-8674(02)00620-7,)

[33] T. E. Fisher, A. F. Oberhauser, M. Carrion-Vazquez, P. E. Marszalek, J. M. Fernandez 1999, The study of protein mechanics with the atomic force microscope, *Trend Biochem. Sci.*, **24**, 379-384. (doi:http://dx.doi.org/10.1016/S0968-0004(99)01453-X)

[34] A. A. Griffith 1920, The Phenomenon of Rupture and Flow in Solids, *Phil. Trans. R. Soc. A*, **221**, 163.

[35] M. J. Harrington, S.S. Wasko, A. Masic, F.D. Fischer, H.S. Gupta, and P. Fratzl (2012), Pseudoelastic behaviour of a natural material is achieved via reversible changes in protein backbone conformation, *J. R. Soc. Interface*, **9**, 2913. (doi:10.1098/rsif.2012.0310)

[36] C. O. Horgan, G. Saccomandi, *A molecular-statistical basis for the Gent model of rubber elasticity* J. of Elasticity, **68**, 167–176 (2002).

[37] J. Hsin, J. Strümpfer, E.H. Lee, K. Schulten 2011, Molecular Origin of the Hierarchical Elasticity of Titin: Simulation, Experiment, and Theory, *Ann. Rev. Biophys.*, **40**, 187-203. (doi:0.1146/annurev-biophys-072110-125325)

[38] S.K. Jha, J.B. Udgaonkar 2010, Free energy barriers in protein folding and unfolding reactions, *Curr. Science*, **99**, 457–475.

[39] T. Kajander, A.L. Cortajarena , E.R.G. Main, S.G. J. Mochrie , and L. Regan 2005, A New Folding Paradigm for Repeat Proteins, *J. Am. Chem. Soc.*, **127**, 10188–10190. (doi:10.1021/ja0524494)

[40] Kazakevicuite-Makovska and H. Steeb 2011, *Procedia Engineering*, **10**, 2597. (doi:http://dx.doi.org/10.1016/j.proeng.2011.04.432)

[41] Kearsley E.A. (1989) Strain invariants expressed as average sStretches, *J. Rheol.* **33** 757–760;

[42] M.S.Z. Kellermayer, S.B. Smith, H.L. Granzier, C. Bustamante 1997, Folding-Unfolding Transitions in Single Titin Molecules Characterized with Laser Tweezers, *Science*, **276**, 1112. (doi: 10.1126/science.276.5315.1112)

[43] D. J. Lacks 2005, Energy Landscape Distortions and the Mechanical Unfolding of Proteins, *Biophysical Journal*, **88**, 3494-3501. (doi:http://dx.doi.org/10.1529/biophysj.104.051953)

[44] E.H. Lee, J. Hsin, O. Mayans, K. Shulten 2007, Secondary and Tertiary Structure Elasticity of Titin Z1Z2 and a Titin Chain Model, *Biophys. J.*, **93**, 1719–1735. (doi:http://dx.doi.org/10.1529/biophysj.107.105528)

[45] W.A. Linke, A. Grützner 2008, Pulling single molecules of titin by AFM-recent advances and physiological implications, *Pflügers Archiv - European Journal of Physiology*, **456**, 101–115. (doi:10.1007/s00424-007-0389-x)

[46] S. Lv, D.M. Dudek, Y. Cao, M.M. Balamurali, J. Gosline, H. Li 2010, Designed biomaterials to mimic the mechanical properties of muscles, *Nature*, **465**, 69–73. (doi:10.1038/nature09024)

[47] D. E. Makarov 2009, A Theoretical Model for the Mechanical Unfolding of Repeat Proteins, *Biophys. J.*, **96**, 2160-2167. (doi:http://dx.doi.org/10.1016/j.bpj.2008.12.3899)

[48] F. Manca, S. Giordano, P.L. Palla, F. Cleri, and L. Colombo 2013, *Phys. Rev. E*, **87**,032705. (doi:10.1103/PhysRevE.87.032705)

[49] M. Carrion-Vazquez, A.F. Oberhauser, S.B. Fowler, P.E. Marszalek, S.E. Broedel, J. Clarke, and J.M. Fernandez 1999, *Proc. Nat. Acad. Sci.*, **96**, 36943699 (1999). (doi:10.1073/pnas.96.7.3694)

[50] J.F. Marko, E.D. Siggia 1995, *Macromol.*, **28**, 8759–8770. (doi:10.1021/ma00130a008)

[51] C. Miehe, S. Gktepe, F. Lulei, 2004, *J. Mech. Phys. Solids.*, **52**, 2617–2660.

[52] L. Mirny, E. Shakhnovich 2001, Protein Folding Theory: From Lattice to All-Atom Models, *Annual Review of Biophysics and Biomolecular Structure*, **30**, 361–396, (doi:10.1146/annurev.biophys.30.1.361)

[53] A. Miserez, S.S. Wasko, C.F. Carpenter, J.H. Waite 2009, Non-entropic and reversible long-range deformation of an encapsulating bioelastomer, *Nat. Mater.*, **8**, 910. (doi:10.1038/nmat2547)

[54] N. Nakagawa, M. Peyrard 2006, The inherent structure landscape of a protein, *Proc. Nat. Acad. Sci.*, **103**, 52795284. (doi: 10.1073/pnas.0600102103)

[55] A. F. Oberhauser, P. R. Marszalek, H. P. Erickson, J. M. Fernandez 1998, The molecular elasticity of the extracellular matrix protein tenascin, *Nature*, **393**, 181–185. (doi:10.1038/30270)

[56] E. Oroudjev, J. Soares, S. Arcidiacono, J.B. Thompson, S.A. Fossey, and H.G. Hansma 2002, *Proc. Nat. Acad. Sci*, **99**, 6460–6465, (doi:10.1073/pnas.082526499)

[57] G. Puglisi, L. Truskinovsky 2002, A mechanism of transformational plasticity, *Cont. Mech. Therm.*, **14**, 437–457. (doi:10.1007/s001610200083)

[58] G. Puglisi, L. Truskinovsky 2005, Thermodynamics of rate-independent plasticity, *J. Mech Phys. Sol.*, **53** , 655–679. (doi:http://dx.doi.org/10.1016/j.jmps.2004.08.004)

[59] Puglisi G., Truskinovsky L. (2013). Cohesion-decohesion asymmetry in geckos. *Phys. Rev. E*, 87 (3), art. no. 032714.

[60] F. Maddalena, D. Percivale, G. Puglisi, L. Truskinovsky 2009, Mechanics of reversible unzipping *Continuum Mech. Thermodyn.*, **21** , 251–268. (doi:10.1007/s00161-009-0108-2)

[61] G. Puglisi, L. Truskinovsky 2013, Cohesion-decohesion asymmetry in geckos *Phys. Rev. E*, **87** , 032714. (doi:10.1103/PhysRevE.87.032714)

[62] Z. Qin and M.J. Buehler 2010, Cooperative deformation of hydrogen bonds in beta-strands and beta-sheet nanocrystals, *Physical Review E.*, **82**, 061906. (doi:10.1103/PhysRevE.82.061906)

[63] H.J. Qi, C. Ortiz, M.C. Boyce 2006, Mechanics of Biomacromolecular Networks Containing Folded Domains, *Trans. ASME, Jnl. Engineering Materials and Technology*, **128**, 509–518.

[64] R. Raj, P.K. Purohit 2011, *J. Mech. Phys. Sol.*, **59**, 2044-69. (doi:http://dx.doi.org/10.1016/j.jmps.2011.07.003)

[65] M. Rief, F. Oesterhelt, B. Heymann, H.E. Gaub 1997, Single Molecule Force Spectroscopy on Polysaccharides by Atomic Force Microscopy, *Science*, **275**, 1295–97. (doi:10.1126/science.275.5304.1295)

[66] M. Rief, J. M. Fernandez, H. E. Gaub 1998, Elastically Coupled Two-Level Systems as a Model for Biopolymer Extensibility, *Physical Review Letters*, **81**, 4764. (doi:10.1103/PhysRevLett.81.4764)

[67] M. Rief, M. Gautel, F. Oesterhelt, J. M. Fernandez, H. E. Gaub 1997, Reversible Unfolding of Individual Titin Immunoglobulin Domains by AFM, *Science*, **276**, 1109-1112. (doi:10.1126/science.276.5315.1109)

[68] M. Rief, H. Grubmüller 2002, Force Spectroscopy of Single Biomolecules, *Chemphyschem*, **3**, 255-261. (doi:10.1002/1439-7641)

[69] F. Ritort 2006, Single-molecule experiments in biological physics: methods and applications, *J. Phys, Cond. Matt.*, **18**, R531. (doi:10.1088/0953-8984/18/32/R01)

[70] F. Ritort, C. Bustamante, I. Tinoco 2002, A two-state kinetic model for the unfolding of single molecules by mechanical force, *Proc. Nat. Acad. Sci.*, **99**, 13544. (doi:10.1073/pnas.172525099)

[71] M. Rubinstein, R.H. Colby (2003) Polymer Physics. Oxford University Press.

[72] I. Schwaiger, C. Sattler, D.R. Hostetter, M. Rief, 2002. The myosin coiled-coil is a truly elastic protein structure. *Nature Mat.*, **1**, 232–235.

[73] H. Shulhaa, C.W.P. Foob, D.L. Kaplanb, V.V. Tsukruka, 2006, Unfolding the multi-length scale domain structure of silk fibroin protein, *Polymer*, **47**, 5821–5830. (doi:http://dx.doi.org/10.1016/j.polymer.2006.06.002)

[74] S.B. Smith, Y. Cui, C. Bustamante 1996, Overstretching B-DNA: the elastic response of individual double-stranded and single-stranded DNA molecules, *Science*, **271**, 795 (1996).

[75] D. B. Staple, S.H. Payne, A. L. C. Reddin, H. J. Kreuzer 2008, Model for Stretching and Unfolding the Giant Multidomain Muscle Protein Using Single-Molecule Force Spectroscopy, *Phys. Rev. Lett.*, **101**, 248301. (doi:10.1103/PhysRevLett.101.248301)

[76] Y. Termonia 1994, Molecular Modeling of Spider Silk Elasticity, *Macromolecules*, **27**, 7378. (doi:10.1021/ma00103a018)

[77] Treloar L. R. G. (1975) The Physics of Rubber Elasticity Oxford University Press, Oxford and New York.

[78] M. Vendruscolo, E. Paci 2003, Protein folding: bringing theory and experiment closer together, *Curr Opin Struct Biol.*, **13**, 82–87. (doi:http://dx.doi.org/10.1016/S0959-440X(03)00007-1,)

[79] K. Wang 1996, Titin/connectin and nebulin: giant protein rulers of muscle structure and function, *Adv. Biophys.*, **33**, 123-134.

[80] H. Li, W.A. Linke, A.F. Oberhauser, M. Carrion-Vazquez, J.G. Kerkvliet, H. Lu, P. E. Marszalek, J.M. Fernandez 2002, Reverse engineering of the giant muscle protein titin, *Nature*, **418**, 998-1002. (doi:10.1038/nature00938)

[81] W.A. Linkea, M. Kulkea, H. Lib, S. Fujita-Beckerc, C. Neagoea, D.J. Mansteinc, M. Gauteld, J.M. Fernandez 2002, *J. Struct. Biol.*, **137**, 194–205. (doi:http://dx.doi.org/10.1006/jsbi.2002.4468)

[82] Šilhavý M. (1997). The Mechanics and Thermodynamics of Continuous Media, Springer.

[83] Shulha H ., Foo C., Kaplan D.L., Tsukruk V.V. (2006). Unfolding the multi-length scale domain structure of silk fibroin protein. *Polymer* 47 (2006) 5821–5830.

[84] P. D. Wu and E. Van der Giessen 1993, *J. Mech. Phys. Solids.*, **41**, 427–456.

[85] B. Zhang, J.S. Evans 2001, Modeling AFM-Induced PEVK Extension and the Reversible Unfolding of Ig/FNIII Domains in Single and Multiple Titin Molecules, *Biophys. J.*, **80**, 597–605. (doi:http://dx.doi.org/10.1016/S0006-3495(01)76040-7)

[86] Ziegler, H., (1983). An Introduction to Thermomechanics, North-Holland, Amsterdam, ISBN 0-444-86503-9

[87] C. Miehe, S. Goektepe and F. Lulei (2004), A micro-macro approach to rubber-like materials - Part I: The non-affine micro-sphere model of rubber elasticity. *J. Mech. Phys. Sol.*, **52**, 2617– 2660.

[88] C. Truesdell, W. Noll (1965) The Non-Linear Field Theories of Mechanics. Handbuch der Physik, Bd. III/3, Springer Berlin